COMPUTATION OF RELATIVE PERMEABILITY FUNCTIONS IN 3D DIGITAL ROCKS BY A FRACTIONAL FLOW APPROACH USING THE LATTICE BOLTZMANN METHOD

Giuseppe De Prisco[1], Jonas Toelke[1], and Moustafa R Dernaika[2]
[1]Ingrain Inc., Houston, and [2]Ingrain Inc., Abu Dhabi

ABSTRACT

Digital rock physics (DRP) combines advanced 3D imaging techniques such as X-ray computed tomography (CT) scanning or focused ion beam scanning electron microscopy (FIB-SEM), segmentation algorithms to create a digital representation of the rock and advanced numerical methods to evaluate electrical, elastic, fluid flow and other properties of the rocks.

A difficult problem in the numerical evaluation of relative permeability is to replicate the exact saturation sequences performed in SCAL experimental procedures including primary drainage and imbibition. In order to replicate these cycles, it is essential to define appropriate inlet and outlet boundary conditions to mimic the right flow field at the entrance and exit of a volumetric fraction of the plug, potentially located in any position inside the plug itself. Moreover, in order for a digital sample to be a representation of the whole plug, or only part of it in case of a plug with multiple flow units, it is important to make sure that the digital sample is a Darcian sample such that permeability can be defined and the sample is a volumetric representation of the plug. We present an approach to simulate fractional flow in a 3D digital rock by direct numerical simulation of the Stokes flow of two immiscible components through the rock. We use an improved method of the lattice Boltzmann method (LBM) to simulate the complex fluid movement through the rock that includes interfacial tension, wettability and viscous effects. Advanced boundary conditions are presented that allow the injection of varying fractional flow in a displacement process. A robust and simple way to verify Darcy's law and to define a representative sample is presented. Primary drainage and imbibition cycles are performed on a carbonate sample, and the results are in good agreement with the experiments. The simulations are run on high performance computing (HPC) hardware to cope with the enormous computational load.

INTRODUCTION

Over the last two decades excellent progress has been made in areas of pore scale modeling, e.g. in the representation of the rock itself and in the description of the pore-scale physics. Three-dimensional images of rocks can be generated from micro- or nano-CT images over a wide range of resolutions. Still, the a priori prediction of two-phase

flow functions is a challenging topic. In [1] it is stated that the predictive capability of pore network models is of limited use because the number of parameters that go into the modeling is larger than the number of parameters contained in the two-phase flow functions. The authors agree with the statement in [1] that the wetting assignment is the most complex and least validated stage of digital rock physics, but they are also convinced that by using the actual geometry of the pore space, by staying as close as possible to the physics and by reducing the amount of modeling, the number of parameters can be reduced and therefore the predictive capabilities of pore scale models can be enhanced. Another challenging problem is, as underlined in [2], the definition of appropriate boundary conditions: it is explicitly stated that relative permeability using steady-state simulations has proved to be particularly difficult because inlet/outlet condition are not known, and the solution of this problem can provide a direct way to compute digitally relative permeability. The authors agree with this point as well, and they propose with this work an efficient and robust solution to the boundary condition problem (Patent Pending). Another difficulty in digital rock physics is to define a representative elementary volume (REV) of the plug. Even though many solutions to define a representative volume (RV) have been presented in the literature[3, 4, 5], there are no robust methods today that can screen digital subsamples in a fast way with respect to Darcian flow and that can define a REV. Even though this work is not centered on this problem, the authors are giving an example of a fast and robust method to select a Darcian REV (Patent Pending).

LATTICE BOLTZMANN METHOD

In the last two decades the LBM has matured to an alternative and efficient numerical scheme for the simulation of fluid flows and transport problems [6]. The scheme is particularly successful in transport problems involving interfacial dynamics, complex and/or changing boundaries and complicated constitutive relationships. This is the case for the direct numerical simulation of multi-component and immiscible multiphase fluid flows in porous media. We choose a recently developed LB scheme [7]. One feature of this model is a local collision operator, so no gradients have to be computed as in other models. This is especially helpful for flow in porous media with narrow throats and for implementation on HPC hardware. Another feature of this model is a new approach for the separation of immiscible fluid phases, which avoids lattice pinning but still gives sharp interfaces. In addition, a completely new method for implementing contact angles has been developed. The contact angle between the normal of the boundary and the normal of the fluid-fluid interface is set by a local, nonlinear optimization procedure. The contact angle can be distributed locally in space according to mineralogy and time to account for aging effects [8]. In fact, the wettability ranges from how the wettability is distributed over the surface of the rock and how it does change with time and different stages in an experiment. The wettability of the reservoir rock is known to have a profound effect on multi-phase petrophysical properties and the literature on this is vast.

HIGH PERFORMANCE COMPUTING

The numerical solution of the Partial Differential Equations (PDEs) describing two-phase displacement in the pore scale is an extremely demanding task due to complex physics with moving interfaces in a highly complex pore geometry, time dependent boundary conditions, the use of feedback methods, a huge number of degrees of freedom and due to demanding parameters for the numerical scheme.

In order to solve the problem on large rock samples, we implemented the LB algorithms for multiple Graphics Processing Units (GPU). GPUs offer a very high memory bandwidth and computational power. Current GPUs have thousands of cores on a chip. Tools like the "Compute Unified Device Architecture" (CUDA) and "Open Computing Language" (OpenCL) allow accessing the computational power through inherently parallel programming concepts. Since GPUs allow very fine grained parallelism, each voxel is handled by an individual thread (where only the computational nodes are allocated). Thousands of threads can be launched in parallel on a single GPU. Between GPUs the computational domain is split along the flow direction in slices. Each slice is handled by one GPU. The data between the GPUs is exchanged by using the message passing interface (MPI). Since modern GPUs allow to transfer data and to compute simultaneously, it is possible to implement communication hiding so that we can reach a very high efficiency [9, 10]. For a typical simulation with a matrix of 500x500x1000 voxels with flow direction in z we use around 50 GPUs in parallel.

Numerical Calculation of Relative Permeability

Laboratory SCAL studies for measuring relative permeabilities are performed by different methods. One of the preferred methods is to initially saturate the plug with simulated formation water and drain it by a porous plate to Swi. The plug is then flushed with live-oil and aged under reservoir conditions for a period of time. Relative permeability is then determined by the steady state method at reservoir conditions. The water fraction is increased in steps from zero to one. Eventually the water rate is increased at the end (bump flood). Differential pressure and oil production are measured during the experiment together with in situ saturation profiles and the relative permeability is calculated with Darcy's law at each steady state rate.

The relative permeability depends on many factors including fluid composition and surface mineralogy, interfacial tension, viscosity contrast between the fluid phases, velocities of the fluids, saturation level of the fluid in the pores, structure and connectivity of the pores and the pore space geometry. These parameters may vary in space and time and hence may vary with the resulting fluid state and composition changes during production of fluids. Saturation history also has a major effect on relative permeability and one major consequence of this is the fact that the relative permeability-saturation relationship exhibits hysteresis effect between drainage and imbibition processes.

A first attempt to compute relative permeability was published by Ferreol and Rothman [11] and was used subsequently in several studies. The porous medium was artificially converted into a periodic system by mirroring and the system was driven by a volume

force. In such a system, at least three problems arise. First, the volume force has to be small enough not to introduce forces which are comparable to capillary forces over a typical feature size. This would lead to an artificial deformation of the fluid-fluid interface and yield incorrect results. Moreover, the iso-lines of the field generated by an external body force can be different from a field generated by a pressure difference when multiple fluids are present. Secondly, the two-fluid phases are distributed in an artificial manner and do not represent the correct initial conditions: distribution of saturation is a first order variable to calculate relative permeability. Thirdly, it is not possible to compute saturation endpoints with a method that has to pre-define saturations of the two phases. In [12] it is claimed that by keeping a previous fluid distribution state and by injecting fluid into the model according to the direction of change in saturation hysteretic behavior can be reproduced. An unsteady state relative permeability process based on the Johnson, Bossler, and Naumann (JBN) method was proposed in [12]. There, relative permeabilities are constructed by a single displacement flood and an indirect computation method. Larger deviations from the steady state method are observed and it is also claimed that relative permeabilities can only be derived for a limited saturation range, which is a limitation of indirect unsteady state techniques in general.

To produce a better method, we developed a digital setup that adheres closely to the experimental procedure where relative permeability curves are computed by a displacement process using different fractional flows. Here, two main obstacles have to be overcome [2]. The first one is to implement suitable multiphase boundary conditions at the inlet and the outlet of the plug. The second one is to adjust the flow rates of the fluids in such a way that a certain flow ratio is set and at the same time iso-pressure conditions are given at the inlet. Our approach addresses these issues and is different from other attempts to compute relative permeability with the LBM. First, a method to judge how representative a digital sample is in terms of Darcy flow is presented.

Darcian sample and Representative Elementary Volume (REV)
The description used for the simulation of flow in a porous medium on the macro-scale is derived from Darcy's Law. To derive Darcy's law from the Navier-Stokes equations Gray's decomposition of scales has to be applied, e.g. $P = \bar{P} + \tilde{p}$. $\bar{P}$ is an averaged quantity (in this case pressure) that is supposed to be "well behaved" over the averaging integral scale (that can be the length scale of the sample, like the transverse or longitudinal dimension) [13]. The quantity $\tilde{p}$ is the fluctuating part of the pressure: it represents the variation of the function. A hypothesis is that the averaged quantities do not change on the small scales where the fluctuating part is allowed to have small variation. To derive Darcy's law, together with Gary's decomposition, a volume average operation must be applied to the Navier-Stokes equations. In this case one obtains the average of gradients of fields while it is the gradient of the averaged quantities that is desired. It can be proved easily that the two operators (gradient and average) commute when applied to functions that do not change rapidly over the averaging length scales, in particular when the porosity is uniform. When a digital sample is selected there is a possibility that variation of porosity or pressure gradient along the flow direction

invalidates assumptions about Darcy Flow. This is especially true for highly heterogeneous samples such as those found in real world rock formations.

A way to make sure that permeability can be defined through Darcy's law is to apply a transformation F that maps the pore-space within the sample to a distribution of variation of properties such as porosity, the ratio of surface over pore-volume and other local Minkowski functions [5]. The transformation F(l) depends on a linear dimension l that can be chosen arbitrarily. The moments of the distribution (average, variance, skewness and kurtosis) give an indication of the heterogeneities present in the sample with respect to the length scale l. Zero average and variance for the distribution obtained by F(l) means that the rock has a periodic structure with period l of the specific properties or functions.

Figure 1 shows the distribution of the variation of surface over pore-volume along the flow direction normalized by the average of the whole sample for a length scale l which is 2.5 times smaller than the linear dimension L of the whole sample. A value of one on the abscissa means that the variation of surface over pore-volume for a subsample with linear dimension of l=L/2.5 is 100% with respect to the average value of the whole sample. In the case of Figure 1 the distribution has the first order moment very close to the variation of the original whole sample (the circle in Figure 1) and it is close to zero. The variance of the distribution is relatively small as well. The variations do not change rapidly within the majority of the sub-samples, so a well behaved pressure gradient is expected within this scale that can be defined as "integral scale" for the sample. This is of course true for the original size of L as well and for any intermediate length scale between L and L/2.5. The same results were obtained for porosity. Therefore a sample with linear dimension of L/2.5 can represent the original sample in terms of porosity and permeability, so it can be a RV. To find the scale of the REV the length scale l has to be iteratively decreased until the moments of the distribution start to increase with respect to the value of a larger length scale. We find that for a Darcian sample, the transformation F(l) always starts with a Gaussian-like distribution for a length scale l relatively close to the original size L and starts to deviate for a certain small length scale l.

A different case is depicted in Figure 2 where large heterogeneities on the considered scale L/2.5 are present. This scale cannot be considered an integral scale because large fluctuations of quantities like pressure and porosity could be present. The sample is rejected for the numerical evaluation of properties like permeability and porosity unless a larger sample is available to characterize that flow unit.

Boundary Conditions

The selection of boundary conditions can significantly affect the time required for computation, the accuracy of results and the stability of the simulation. This is especially true for immiscible multi-phase or multi-component simulations. Difficulties arise from the fact that the pressure and distribution of phases and velocities at the inlet of the digital sample are unknown, and these conditions must be established such that they mimic the physical conditions. We propose a method where we combine a special setup for the inlet area for the injection of a wetting and non-wetting fluid into the pore space and a process

control application to achieve quasi-steady state flow at different fractional flow rates of both fluids.

The inlet face of a sample in drainage or imbibition mode (when both phases are injected), as shown in **Error! Reference source not found.**, has dark gray (red in color) areas in the center part of each pore through which the non-wetting phase enters and light gray (light blue in color) annular areas through which the wetting phase enters. The rock solid matrix is represented in medium gray (or dark blue in color). This inlet was designed digitally to assign wetting and non-wetting fluid distribution in an annular way according to the shape of the pores. The area for the wetting fluid is first distributed at the inlet face of the pores as layers of voxels. The percentage of the wetting/non-wetting fluid area may be increased by adding more voxels. This situation approximates the real flow behavior as the wetting fluid has an attraction to the solid surfaces in the rock and the non-wetting fluid will stay in the center of the pore space. The ratio of these two areas can be adjusted for low or high flow ratios of the two fluids. Each of the two fluids is subjected to a different pressure at the inlet that is setting the target flow rate. An initial value for Pw, the pressure exerted on the wetting fluid, and Pn, the pressure exerted on the non-wetting fluid can be obtained from Darcy's law and from initial guesses for the relative permeability curves (for example obtained with quasi-static simulation [2]) in the case the sample is filled with both phases at the start of the simulation. Corrections are made to the inlet pressures, Pw and Pn, with a closed-loop feedback control system in such a way that the target flow rates QwT and QnT are achieved. For each time increment that feedback control corrections are made, the values of the two flow rates are stored and a moving time or weighted time average of the fluxes is calculated. The weighted average can be an arithmetic weighted average, a geometric weighted average, or a harmonic weighted average, a simple rolling average or an exponentially weighted moving average. The pressures Pw and Pn are set independently by two independent feedback control algorithms.

The present work uses a negative feedback control algorithm as shown in . The errors Ew and En are calculated by subtracting the actual value, QW and QN, from the target value, QwT = QT x Fw and QnT =QT x Fnw, where Fw and Fnw are the desired flow fractions for the wetting and non-wetting phases. Two proportional–integral–derivative (PID) control algorithms are used to control the flow of each phase. In the case of PID control the integral and derivative of the errors Ew and En are calculated at each time step t in a way to define the output of the PID controller, πw and πn. The output of the PID control is used to define the variation of the pressure from its initial value so that, for each phase, the new pressure is Pw = Pi + Pi*πw, and Pn= Pi + Pi*πn, where Pi*π is the variation of the pressure each time the controller is activated. The initial pressure value sets the scale of both the pressure and its variation. For example, for the wetting phase, the PID control loop can comprise an input error Ew and output a new inlet pressure, Pw, wherein Pw = Pi + Pi*πw, Pi = the initial pressure set at the beginning of the simulation, πw = f(Ew) such as $K_P * Ew + K_I \int Ewdt + K_D \frac{dEw}{dt}$, where K_p = proportional control constant, K_I

= integral control constant (dimension of 1/time), and K_D = derivative control constant (dimension of time). PID control loops are tuned by methods such as manual tuning, Ziegler-Nichols, Cohen-Coon, and other methods.

A schedule can be setup to run the numerical experiment. First, an initial state (e.g. desaturation to Swi) that can be obtained by a porous plate simulation or any other method is loaded. Now schedules with different fractional flow rates can be defined, e.g: Swirr by porous plate or drainage by flooding, imbibition relative permeability and optionally secondary drainage relative permeability. Another schedule is drainage relative permeability - imbibition relative permeability and optionally - secondary drainage relative permeability.
Depending on the fractional flow rate, the viscosity ratio and the capillary pressure, the areas Aw and An can be adjusted to minimize the spurious influence of the approximated inlet condition. As an example, for low values of Fn/(Fn+Fw), the area An may need to be reduced and Aw increased. The pressure at the outlet condition is set according to the predominant phase at the start of the simulation: the phase with the largest saturation is set to a reference pressure (e.g. zero) and the pressure of the other phase is set automatically through a capillary pressure jump condition. The distribution of the phases at the outlet is extrapolated in space from the upstream plane.
After all flow rates, pressures and saturations have been calculated, imbibition and drainage relative permeabilities can be calculated for the water saturations corresponding to each fractional flow state.

RESULTS AND DISCUSSIONS

We consider Sample #33 from a previous study [14]. It is a Middle Eastern carbonate from the Orbitolinid, Skeletal Wackestone (OSW) lithofacies. The OSW lithofacies implies deposition in low-energy, open platform below fair weather wave base, possible middle ramp. The measured porosity fraction for this plug was 0.24(NMR)/0.23(Helium). The absolute permeability was measured to be 0.82 mD, the obtained Swi fraction after a porous plate experiment was 0.124 and the effective oil permeability at Swi after ageing was 0.78 mD. We scanned a sample of the core at a voxel resolution of 65 nm which resolves the pore system. The DRP-derived porosity fraction and absolute permeability (in the direction of flow) were determined as 0.238 and 1.3mD, respectively. These values are slightly higher than the laboratory measured results. This must be due to the heterogeneity in the rock and the fact that DRP data was obtained on very small fraction of the original plug sample. The number of voxels in each direction of the reconstructed sample (a cube) is 500. The digital NMR PSD, MICP PTSD and drainage/imbibition Pc curves are in good agreement with the experimental data, and the comparisons are given in another paper of this conference [15]. The sample was subjected to the REV procedure described earlier and it showed a relatively narrow distribution close to zero (see Figure 1, right). With these checks which involve experimental data (MICP and optionally NMR) we make sure that we have a representative sample of the rock. The fluids are formation water with a viscosity of 0.33 cP and live oil with a viscosity of 0.28 cP under reservoir conditions. The digital porous plate experiment gives a value of Swi in good agreement with the experiment as shown in [15]. The actual geometry of the sample is

shown in Figure 1 (left), and the experimental imbibition Kr curves are given by the red curve in Figure 5. Results are reported with consideration of Ca number (U $\mu \sigma^{-1}$) and viscosity ratio of the two fluids ($\mu_w \mu^{-1}_{nw}$), that are sufficient numbers of non-dimensional parameters to describe the physics. The Ca number is set in order to have a system dominated by capillary forces (typical in the experimental procedures) and to have an acceptable turnaround time according to a commercial applicability of the calculation (A lower Ca number directly translates to a higher computational effort). The range for capillary dominated flows is dependent on the morphology and geometry of the rock and is usually between Ca=10^{-4}-10^{-6}. We choose a capillary number that gives an acceptable turnaround time while keeping the flow capillary dominated. For a Ca of 10^{-5} the flow rate in the sample is in the order of 10^{-6} cc/s. The viscosity ratio was fixed according to the experiments. A contact angle θ=30° was fixed for the primary drainage (experiments not available) and θ=135 for the primary imbibition. In this work we did not modify the values for the contact angles and it should be seen as a possibility to enhance the prediction of the flow properties of the rock rather than a tuning-trial-and-error work in order to match the experimental results. The authors believe that a mixed wettability porosity network for the primary imbibition is more appropriate to simulate the physics of multiphase flow in porous media. Small pores and pores behind very small throats are typically not invaded by the oil during the primary drainage, so the small pore space features remain water wet in a following aging process and in the following primary imbibition steps. The focus of this paper is not on mixed wet systems, but the authors are preparing a detailed paper on that topic. Shortly, to obtain the distribution of phases and to assign the contact angles at the boundaries of the porous medium for a mixed wet system a digital MICP or Pc drainage up to a final pressure is run [15]. A water wet contact angle (30°) is assigned to the boundaries of the non-invaded pore space and a larger contact angle (135° in this case) to the remaining boundaries. In this way the aging can be mimicked and a mixed-wet system can be obtained. In the case reported here we used the digital MICP.

Relative Permeability
For the numerical calculation we performed a primary drainage relative permeability starting from a water filled sample. The contact angle was set to θ=30 (uniform wettability), and the capillary number (Ca) was set to 2.4 10^{-5}. The fractional flow of oil was increased in steps until a complete flooding with oil was achieved. Since Swi in a laboratory experiment depends strongly on the number of pore volumes injected and the capillary number (Ca), we used three different flow rates for the last point of the drainage cycle (bump flood) for a fixed number of pore volumes injected. Table 1 lists Swi values obtained by oil flood simulations for different Ca numbers and after a fixed number of iteration, that are equivalent to a length of physical time. The flow rate corresponding to Ca=9.5 10^{-5} and 16 pore volumes (corresponding to 0.052 seconds in the digital sample) had Swi close to the value of the porous plate experiment. The corresponding relative permeability of the primary drainage with Ca=2.4 10^{-5} and Ca of the last point (bump flow) 9.5 10^{-5} is the black curve in Figure 5. This curve is therefore constructed from two different Ca values, and this is the reason for the inflection seen at around 50%

saturation. The Ca number was increased such that the target Swi would be achieved faster. Normally, Swi values are set based on reservoir considerations and can be estimated from early measurements like the mercury injection experiments.

The last point of the drainage is setting the starting point of the imbibition curve. Another possibility to define the starting point of the imbibition is to load the distribution of the phases from the digital porous plate experiment (not applied in this case). The same Ca number, which we first used in primary drainage was set in the following imbibition simulations (i.e. 2.4 10^{-5}). Two scenarios are simulated for the imbibition case: one is related to a uniform contact angle of $\theta=135$; another one is a mixed wet system with a $\theta=30$ for the water wet areas and a $\theta=135$ for the oil wet areas. To underline the differences, two simulations for the imbibition were run: the first used the uniform contact angle (yellow curve in Figure 5). It is evident that there is a discrepancy compared to the experimental curve for low water saturation (apparent in the semi log plot to the right of Figure 5), otherwise there is a good match. The second simulation was run where the areas touching residual water were left water wet. Those areas were detected through the end of the drainage step. With this procedure, the water phase injected at small fractional flow can flow through the water phase wetting the rock in the narrow pore space. This gives a very small water permeability value at the lower water saturation range (green curve in Figure 5). The DRP simulation results show very good match with the experimental curves both for endpoints (Swi, Sor) and the intersection points. The choice of the contact angle in imbibition was not arbitrary. It was actually based on large data set of experimental capillary pressure and relative permeability data. Such choice of the contact angle is not discussed in details in this work and it is the intention of the authors to deal with this interesting subject in a separate publication.

The obtained match between our DRP-derived imbibition relative permeability curve and the experiemntal curve can be seen as an important step towards enhancing the predictive nature of such DRP simulations. The main aim in this work was not really to tune the input parameters to match the experimental data. There has been large effort made in selecting representative digital samples, characterizing wettability and improving the lattice Boltzmann Method.

SUMMARY AND CONCLUSIONS
A newly developed pore scale LBM was introduced to improve the accuracy of the computation of two phase flow relative permeability functions in a carbonate reservoir rock sample. The simulation process can be successful if certain conditions are satisfied. The following conclusions can be made from this work,

1. The new LBM method was implemented on high performance computing hardware (28 GPU's in parallel) which allowed the numerical computations to be carried out on larger rock samples (500^3 in the present cases, and order of 30M iterations for each drainage and imbibition) with complex geometries and narrow throats.

2. The method allowed for sharp interfaces between immiscible fluids, and contact angles were set to account for mixed wettability.

3. Unique simulation conditions were developed to compute steady state relative permeability curves by a displacement process using different fractional flow rates. This was successfully achieved by applying suitable multiphase boundary conditions and flow rates.

4. A numerical evaluation procedure was developed and applied to select Darcian sample and REV.

5. The Digital Rock Physics (DRP) workflow combined experimental data from MICP and NMR to ensure the digital pore space was characterized correctly.

6. Primary drainage and imbibition relative permeability curves were derived from the simulations and reasonable match was reported with imbibition steady state relative permeability curves measured at full reservoir conditions.

7. The workflow followed in this study and the LB simulated results show the possibility to enhance the predictive nature of such DRP simulations for reservoir rock properties and flow behavior.

REFERENCES

[1] K. Sorbie and A. Skauge, "Can Network Modelling Predict Two-Phase Flow Functions?" in *SCA2011-29*, Austin, 2011.

[2] Q. Sheng, K. Thompson, J. Fredrich and P. Salino, "Numerical Prediction of Relative Permeability from MicroCT Images: Comparison of Steady-State versus Displacement Methods," in *SPE Annual Technical Conference*, Denver, 2011.

[3] J. Bear, Dynamics of Fluids in Porous Media, New York: American Elsevier, 1972.

[4] Razavi, Muhunthan and Hattamleh, "Representative Elementary Volume Analysis of Sands Using X-Ray Computed Tomography," *Geotechnical Testing Journal,* Bd. 3, pp. 212-219 , 2007.

[5] P. Oren and S. Bakke, "Process Based Reconstruction of Sandstones and Prediction of Transport Properties," *Transport in Porous Media,* Bd. 46, p. 311–343, 2002.

[6] S. Succi, The Lattice Boltzmann Equation for Fluid Dynamics and Beyond, UK: Oxford University Press, 2001.

[7] J. Toelke, G. De Prisco and Y. Mu, "A lattice Boltzmann method for immiscible two-phase Stokes flow with a local collision operator," *acc. for Publication in Computers and Mathematics with Applications.*

[8] A. Kovscek, H. Wong and C. Radke, "A Pore-Level Scenario for the Development of Mixed Wettability," *AIChE Journal,* Bd. 39, pp. 1072-1085, 1993.

[9] J. Toelke and M. Krafczyk, "TeraFLOP Computing on a Desktop PC with GPUs for 3D CFD," *International Journal of Computational Fluid Dynamics,* Bd. 22, Nr. 7, 2008.

[10] J. Toelke, "Lattice Boltzmann Multi-Phase Simulations in Porous Media using GPUs," GTC2010, 2010.

[11] B. Ferreol and D. Rothman, "Lattice-Boltzmann simulations of flow through Fontainebleau sandstone," *Transport in Porous Media,* Bd. 20, Nr. 1, pp. 3-20, 1995.

[12] T. Ramstad, N. Idowu, C. Nardi and P.-E. Øren, "Relative Permeability Calculations from Two-Phase Flow Simulations Directly on Digital Images of Porous Rocks," *Transport in Porous Media,* 2011.

[13] S. Whitaker, "Flow in porous media I: A theoretical derivation of Darcy's law," *Transport in porous media,* vol. 1, pp. 3-25, 1986.

[14] A. Grader, M. Kalam, J. Toelke, Y. Mu, N. Derzhi, C. Baldwin, M. Armbruster, T. Al Dayyani, A. Clark, G. Bin-Dhaaer Al Yafei and B. Stenger, "A Comparative Study Of Digital Rock Physics And Laboratory SCAL Evaluations Of Carbonate Cores," in *SCA2010-24*, Nova Scotia, 2010.

[15] Y. Mu, Q. Fang, C. Baldwin, J. Toelke, A. Grader, M. Dernaika and Z. Kalam, "Drainage and Imbibition Pc Curves of Carbonate Reservoir Rocks by Digital Rock Physics," in *SCA2012-56*, Aberdeen, Scotland, 2012.

Table 1: Swi for different capillary numbers at 10 million iterations.

Ca	#LB iterations	# porevolume	Kro	Swi
$9.5\ 10^{-5}$	10E6	16	0.80	0.15
$4.8\ 10^{-5}$	10E6	16	0.75	0.21
$2.4\ 10^{-5}$	10E6	12	0.65	0.23
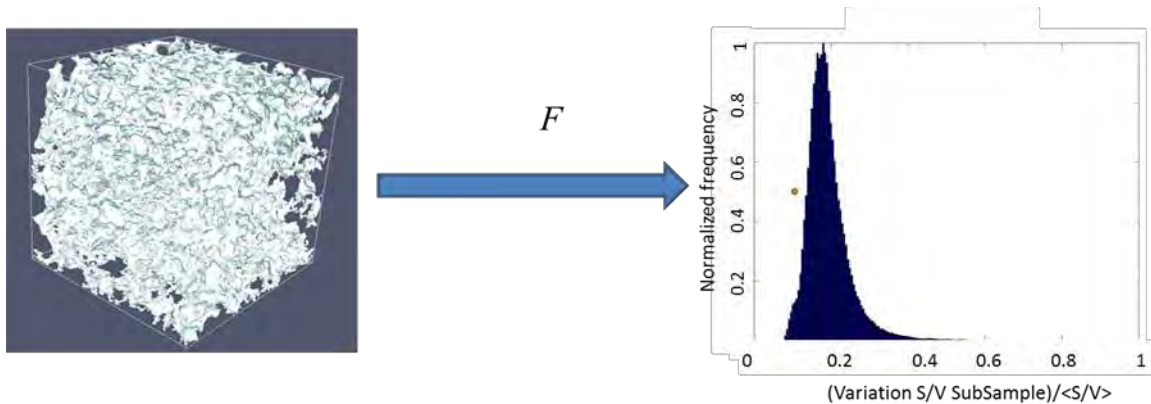
Figure 1: Left: Rock with uniform properties. Right: Distribution of the variation of surface/pore-volume
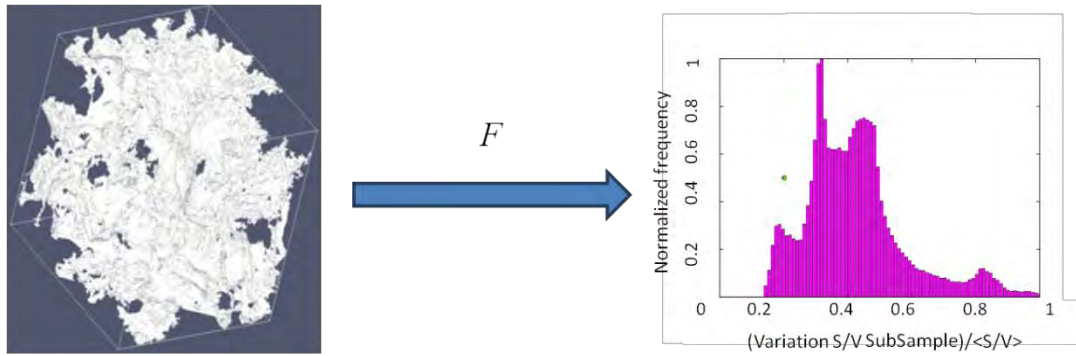
Figure 2: Left: Heterogeneous rock. Right: Distribution of the variation of surface/pore-volume
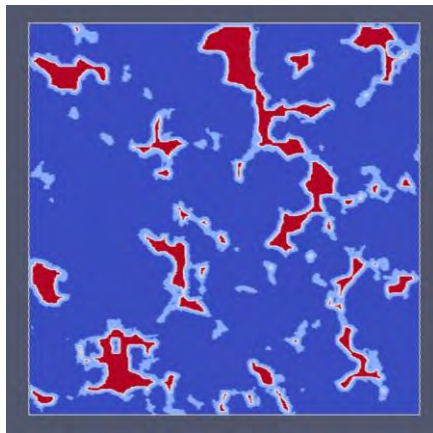
Figure 4: Multiphase inlet-condition: the generation of the inlet is done assigning wetting and non-wetting fluid layer-wise manner. The creation of the wetting area is done by selecting voxels adjacent to the grains and designating them as an area for wetting fluid.
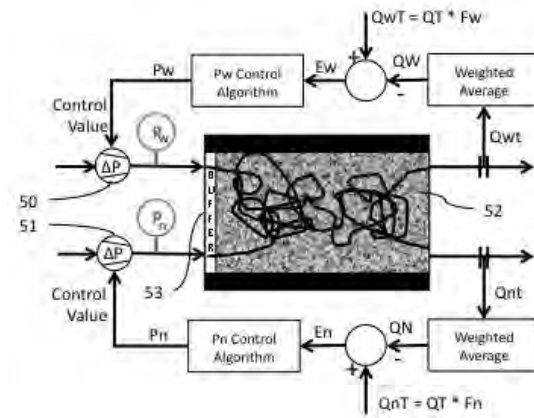
Figure 3: Negative feedback control algorithm for fractional flow.
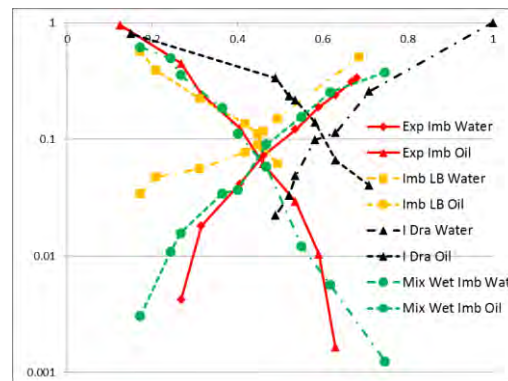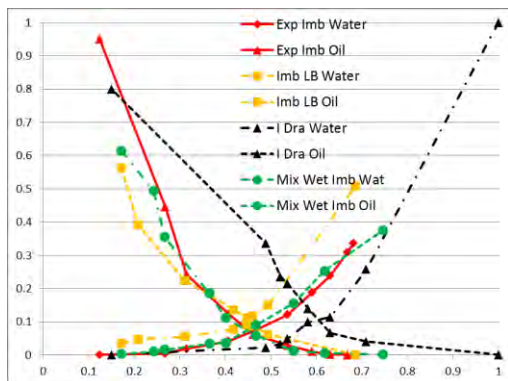
Figure 5: Relative permeability curves for sample #33. Black: Primary drainage simulation, Orange: First imbibition simulation, Red: First imbibition experimental data, Green data: mixed wet approach.